
taskpriors: Enhancing Model Evaluation by Considering the Entire Space of Downstream Tasks

Niket Patel

Department of Mathematics
University of California, Los Angeles
niketpatel@ucla.edu

Randall Balestrieri

Department of Computer Science
Brown University
randall_balestrieri@brown.edu

Abstract

The grand goal of AI research, and particularly Self Supervised Learning (SSL), is to produce systems that can successfully solve *any* possible task. In contrast, current evaluation methods available to AI researchers typically rely on a fixed collection of hand-picked downstream benchmarks. Hence, a large amount of effort is put into designing and searching for large collection of evaluation tasks that can serve as a proxy of our grand goal. We argue that such a rigid evaluation protocol creates a silent bottleneck in AI research. To remedy that, we define a *probabilistic space of downstream tasks* obtained by adopting a distribution of tasks and by defining **Task Priors**¹. Under this view, one can evaluate a model’s performance over the set of all possible downstream tasks. Our framework is the first to provide answers to key questions such as *(i) what is the average performance of my model over all possible downstream tasks weighted by the probability to encounter each task?* or *(ii) what is the variance of my model’s performance across all downstream tasks under the defined Task Priors?* Beyond establishing a new standard for evaluation, we believe that **Task Priors** will accelerate the pace of research in SSL—where downstream task evaluation is the sole qualitative signal that researchers have access to.

1 Introduction

Pretrained backbone models today are released as a single checkpoint, yet in practice they can power millions of distinct downstream tasks: from simple classification and retrieval services to large-scale recommendation, autonomous perception, and more. On HuggingFace alone, top models such as *mobilnetv3*, *clip-vit*, and *bert* can get over 100 million downloads per month [27]. As the number of users and the diversity of applications grows, the space of possible downstream tasks users want their models to perform well on tends toward infinity.

Yet our standard evaluation protocols remain tethered to a small, fixed suite of hand-picked benchmarks—often half a dozen or so datasets (e.g., ImageNet, COCO, GLUE, SuperGLUE, WMT) [12, 19, 16, 25]. Each new benchmark can take months of expert labeling and tens or even hundreds of thousands of dollars to assemble. Even large-scale benchmark suites that aggregate many tasks—such as the Massive Text Embedding Benchmark (MTEB), which spans 56 different evaluation datasets—still represent only a narrow slice of the possible task space [18]. Once built, a static benchmark can only ever probe a tiny corner of the real-world tasks for which a model might be deployed. This disconnect creates a structural bottleneck between the handful of evaluation suites we all agree to evaluate our models on and the effectively infinite variety of tasks practitioners use our models for.

¹<https://github.com/niketp03/taskpriors>, see Appendix C for a simple example.

One way to break this bottleneck is simply to keep spending more time and money on ever-larger benchmarks, but that approach quickly becomes unsustainable. Instead, we propose a surrogate evaluation framework that treats downstream tasks as samples from a well-defined probabilistic space. By adopting a “Task Prior”, a distribution over all possible targets informed by a pretrained feature kernel, we can compute expectations and variances of a model’s downstream performance in closed form, without training new classifiers or designing new benchmarks. We show that this approach provides principled measures of average performance, robustness, and worst-case error across the entire landscape of potential tasks.

Our primary novel contributions in this work are as follows:

- **Task Priors.** We prove that performance on linear probes is equivalent to maximizing the alignment of a kernel with the induced label graph, unifying supervised and self-supervised evaluation. We then formalize the space of downstream tasks as a Gibbs-style distribution over all possible label graphs, making the notion of “any task a user might care about” mathematically explicit.
- **Closed-form Metrics.** From the Task Prior we derive $O(n^2)$ formulas for the expected downstream error and its variance, obviating benchmark curation or probe training.
- **Efficient Task Sampling.** We introduce an $O(n)$ prefix-sampling algorithm that draws realistic classification tasks from the prior, enabling cheap evaluation on many tasks.
- **Empirical Validation.** We find that across a range of backbones, our closed form metrics on kernel align with mean and variance of accuracy of linear probes on a subset of ImageNet. We then introduce a training objective that maximizes this expected task performance while simultaneously minimizing its variance across tasks.

2 Background

Many works aim to capture the performance of representation models primarily by intrinsic quantities about the model’s features. For instance, RANKME measures the *effective rank* of the feature matrix and shows a empirical correlation with average linear-probe accuracy across several tasks [7]. LiDAR argues that a method built on Linear Discriminant Analysis serves as a proxy for downstream performance [23]. More recent works take a broader view, demonstrating that k-NN, few-shot fine-tuning, and clustering evaluations may all disagree in systematic ways [17]. Collectively, these studies show that properties intrinsic to the representation can forecast downstream success, but they still reduce performance to one or two scalar summaries.

A complementary line of work attacks the evaluation bottleneck by increasing the number of test tasks. In NLP, suites such as MTEB (56 embedding datasets) [18] and HELM (42 scenarios, seven axes of measurement) [15] provide broad coverage of downstream tasks. The same trend is exists in vision, with works such as VideoEval packaging twenty diverse video understanding datasets together [13]. While these mega-benchmarks can be quite helpful for practitioners, they remain *finite* and expensive to create. Worse, even a hundred benchmarks sample only a vanishingly small corner of the large task space practitioners can care about.

Our *Task Priors* framework can be viewed as the missing bridge between these two threads. Like intrinsic metrics, it avoids needing a hand curated set of downstream targets, but like conglomerate benchmarks, it explicitly reasons about *many* tasks. Our framework echoes several well-known results from the classical theory of kernels. Notably, the trace term in Theorem 3.3 parallels the Hilbert–Schmidt Independence Criterion (HSIC) of Eq. (4) in [8]. Likewise, the term we get by taking the trace of \mathbf{KG} is precisely the same as “kernel alignment” studied in the context of generalization [5], obtained by flattening each matrix and taking their inner product, as $\langle \mathbf{K}, \mathbf{G} \rangle = \text{Tr}(\mathbf{KG})$.

There are some other related works that attack similar problems. In the computer vision space, VTAB [30] takes a similar distributional view of tasks, but does not precisely characterize the distribution of tasks. Similar to our derivations, [14] proposes a loss function based on the HSIC, which is an interesting avenue for future research.

3 Task Priors

3.1 An Equivalence Between Losses

Traditional downstream evaluation asks, “How well can a linear head map features back to a specific label vector \mathbf{Y} ?” This works when a single, human-defined labeling is the goal, but it scales poorly once we care about many downstream tasks. By recasting supervised objectives in the language of pairwise relations by looking at the sample-sample adjacency matrix \mathbf{G} we leave the “label space” and move into a kernel space where tasks become graphs and models can be represented in terms of the kernel matrix. This shift from comparing features to labels, to comparing features among themselves, allows for us to derive a natural equivalence between supervised and self-supervised objectives, such as those found in contrastive learning [24, 1, 9, 2, 3, 4, 10, 29, 26]. We will leverage this connection to define our Task Prior. To better explain our findings, we first need to introduce the formal definitions of *relative* and *absolute* objectives.

Definition 3.1 (Absolute objective). *An absolute objective compares a prediction of sample \mathbf{x}_n to the target \mathbf{y}_n independently from the other samples.*

Definition 3.2 (Relative objective). *A relative objective compares a $N \times N$ inter-sample relation matrix (e.g., $f_\theta(\mathbf{X})^\top f_\theta(\mathbf{X})$) to a $N \times N$ inter-label relation matrix \mathbf{G} (e.g. $\mathbf{G} = \mathbf{Y}^\top \mathbf{Y}$).*

In many practical settings, rather than focusing solely on self-supervised loss formulations, we are given a pretrained representation $f_\theta(\mathbf{X})$ and wish to assess how well a simple linear head can recover downstream tasks. By solving the unconstrained mean squared error objective for the linear probe, we find that the optimal loss depends only on the kernel matrix $\mathbf{M} = f_\theta(\mathbf{X})^\top f_\theta(\mathbf{X})$ and the label adjacency graph $\mathbf{G} = \mathbf{Y}^\top \mathbf{Y}$:

Let’s denote the input data as the matrix $\mathbf{X} \triangleq [\mathbf{x}_1, \dots, \mathbf{x}_N]$ the targets or labels as the matrix $\mathbf{Y} \triangleq [\mathbf{y}_1, \dots, \mathbf{y}_N]$ where for classification each \mathbf{y}_n is a one-hot vector at the corresponding class, and the model’s prediction as $f_\theta(\mathbf{X}) \triangleq [f_\theta(\mathbf{x}_1), \dots, f_\theta(\mathbf{x}_N)]$. Finally, let’s denote the N -dimensional centering matrix by $\mathbf{H} \triangleq \mathbf{I} - \frac{1}{N} \mathbf{1}_N \mathbf{1}_N^\top$.

Unconstrained linear classifier. We are now minimizing the usual supervised mean squared error between the affinely transformed backbone output $\mathbf{W} f_\theta(\mathbf{X}) + \mathbf{b} \mathbf{1}_N^\top$ and the targets \mathbf{Y} as in

$$\mathcal{L}(\mathbf{W}, \mathbf{b}, \theta) \triangleq \frac{1}{N} \|\mathbf{W} f_\theta(\mathbf{X}) + \mathbf{b} \mathbf{1}_N^\top - \mathbf{Y}\|_F^2 \quad (1)$$

Our goal will be to minimize that loss with respect to \mathbf{W} , \mathbf{b} and to perform some algebraic manipulations to demonstrate how that *absolute* objective—comparing the prediction of sample n to the label of sample n —turns into a *relative* objective—comparing pairwise predictions to pairwise labels. The following derivations do not rely on any assumptions about the input \mathbf{X} , the network f_θ , or the targets \mathbf{Y} , other than that the representations $f_\theta(\mathbf{X})$ are of full rank, which is generally true. We will also denote the Singular Value Decomposition of $f_\theta(\mathbf{X})$ as $\mathbf{U} \Sigma \mathbf{V}^\top$, and the diagonal of Σ as $\sigma_1, \dots, \sigma_K$.

Theorem 3.3. *The optimum of eq. (1) w.r.t. \mathbf{W}, \mathbf{b} can be obtained in closed-form as*

$$\min_{\mathbf{W}, \mathbf{b}, \theta} \mathcal{L}(\mathbf{W}, \mathbf{b}, \theta) = \min_{\theta} -\frac{1}{N} \text{Tr}(\mathbf{V}^\top \mathbf{Y}^\top \mathbf{Y} \mathbf{V}) + \text{cst.} \quad (2)$$

(*Proof in appendix A.1.*)

This theorem shows that the absolute objective from 3.1 is equivalent to the associated relative objective in 3.2. A crucial benefit of eq. (2) is that it only requires \mathbf{G} which could be built from \mathbf{Y} —or without labels at all. For example, in a classification setting, definition 3.1 requires the categorical label for each sample, while definition 3.2 only requires to know which samples are from the same class *but not what that class is*. It is clear that building \mathbf{G} directly instead of \mathbf{Y} is easier and cheaper to get as it reduces the amount of expert knowledge needed.

In the *relative* objective, one no longer tries to predict \mathbf{y}_n from \mathbf{x}_n , but instead tries to make the pairwise comparison of predictions $\mathbf{V} \mathbf{V}^\top$ aligned with the pairwise comparison of labels $\mathbf{Y}^\top \mathbf{Y}$. In particular, we clearly see that the left singular vectors of $f_\theta(\mathbf{X})$ no longer contribute to the loss—as expected since the optimal \mathbf{W} automatically maps them to the left singular vectors of \mathbf{Y} . Hence,

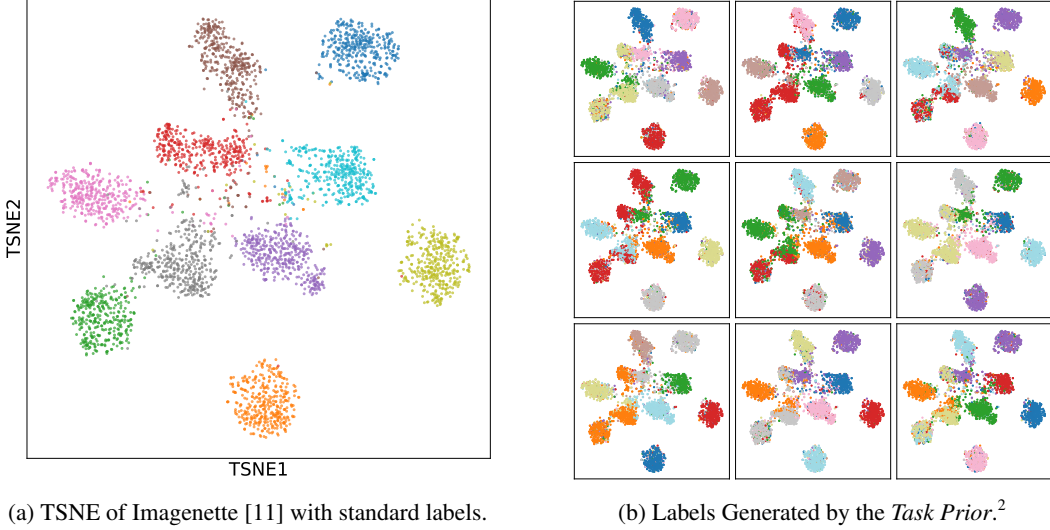


Figure 1: Comparison of the naive way to evaluate a model, only on the specific choice of labels provided with the dataset (Left) with the probabilistic view of targets generated by sampling from the Task Prior, giving us a distribution we can evaluate on (Right).

we are left with the right singular vectors \mathbf{V} of $f_\theta(\mathbf{X})$ and its singular values that appear within \mathbf{D} . Notice that the trace on the right hand side of (2) is not trivial, as \mathbf{V} denotes the truncated SVD, and has orthogonal columns but does not necessarily have orthogonal rows. This is especially true when the number of data points exceeds the feature dimension. So, since we can regard $\mathbf{Y}^\top \mathbf{Y} = \mathbf{G}$ and $\mathbf{V}\mathbf{V}^\top$ is a valid kernel we can write as \mathbf{K} , then we can write our trace as $-\frac{1}{N} \text{Tr}(\mathbf{G}\mathbf{K})$.

Key Takeaway: Objectives that compare samples amongst themselves in a graph structure emerge from considering supervised objectives that compare sample predictions to labels.

3.2 A Distribution Over Target Labels

Building on the kernel view from Theorem 3.3, we now introduce a prior distribution over label graphs \mathbf{G} that reflects the likelihood of different downstream tasks. Instead of manually selecting or training probes on individual benchmarks, we define a measure over all possible \mathbf{G} matrices, weighted by alignment with a pretrained feature kernel \mathbf{K} . This *Task Prior* allows us to compute expectations and variances of kernel alignment scores in closed form, or to efficiently sample realistic downstream targets without training additional classifiers. To achieve this, a practical solution is to define a distribution over possible labelings which assigns a higher probability to more realistic scenarios that might be encountered in real-world applications. This will allow us to look into the average performance of our model, but also have the ability to look into other statistical properties.

Suppose that we have a kernel function that measures similarity between data points $k : \mathbb{R}^D \times \mathbb{R}^D \rightarrow \mathbb{R}$. Let \mathbf{K} then be a kernel matrix corresponding to \mathbf{X} . For the rest of the paper we can assume this is the centered kernel matrix corresponding to the features. Now if we have a graph adjacency matrix \mathbf{G} , we can read off the elements of the product,

$$[\mathbf{G}\mathbf{K}]_{ij} = \sum_{k=1}^N \mathbf{G}_{ik} k(\mathbf{x}_j, \mathbf{x}_k).$$

²Interested readers can experiment with different class counts and temperature settings in this Colab notebook: <https://colab.research.google.com/drive/1qN0goNSH87Acd0Dug-yop7Q0MuT8w1r7>

In particular we can see that the diagonal elements of this matrix is given as follows, where we use $\mathbf{x}_j \sim \mathbf{x}_i$ to mean that \mathbf{x}_j and \mathbf{x}_i are connected in graph \mathbf{G} ,

$$[\mathbf{GK}]_{ii} = \sum_{k=1}^N \mathbf{G}_{ik} k(\mathbf{x}_i, \mathbf{x}_k) = \sum_{\mathbf{x}_k \sim \mathbf{x}_i} k(\mathbf{x}_k, \mathbf{x}_i).$$

Summing over i gives the trace,

$$\text{Tr}(\mathbf{GK}) = \sum_{i=1}^N \sum_{\mathbf{x}_k \sim \mathbf{x}_i} k(\mathbf{x}_i, \mathbf{x}_k),$$

which acts as a global *compatibility score* between the geometry in the label graph \mathbf{G} and the kernel \mathbf{K} . We treat the negative trace, $\mathcal{E}(\mathbf{G}) := -\text{Tr}(\mathbf{GK})$, as the "energy" of a labeling: graphs that connect feature-similar points (high trace of \mathbf{GK}) have lower energy and are therefore more likely. This leads to the naturally to the Gibbs measure

$$\mu(\mathbf{G}) \propto e^{-\mathcal{E}(\mathbf{G})/T} = e^{\text{Tr}(\mathbf{GK})/T},$$

with temperature $T > 0$. As we increase the temperature, this distribution tends towards the uniform distribution on all graphs, and we get more interesting behavior in the low temperature regime. The properties of this distribution enable direction computation of the expectation and higher moments, and enable efficient sampling algorithms which we develop in the sequel.

Definition 3.4. (*Task Prior Distribution*) Given a kernel matrix \mathbf{K} on n data points, and a temperature $T > 0$, we will define the following Gibbs measure on the space of all graphs, \mathbf{G} as:

$$\mu(\mathbf{G}) \propto e^{\frac{\text{Tr}(\mathbf{GK})}{T}}, \quad (3)$$

where we denote by $Z_{T,\mathbf{K}}$ the corresponding partition function.

If we have multiple task prior kernels, $\mathbf{K}_1, \mathbf{K}_2$, then we can compute that $\mu_{\mathbf{K}_1}(G)\mu_{\mathbf{K}_2}(G) \propto \mu_{\mathbf{K}_1 + \mathbf{K}_2}(G)$, giving an easy way to leverage multiple backbones for the task prior distribution.

Although computing exactly the probability of observing a single graph can be quite challenging, as computing the partition function would require 2^{N^2} computations, the specific structure of this probability measure admits a neat factorization on a per-edge level.

Lemma 3.5. Suppose that we consider the Gibbs measures over all graphs \mathbf{G} . Then, the probability of a single edge i, j being present is given by,

$$\mathbb{P}(\mathbf{G}_{i,j} = 1) = \sigma(\mathbf{K}_{i,j}/T), \quad (4)$$

where σ denotes the sigmoid function. Furthermore if $(i, j) \neq (l, k)$, then,

$$\mathbb{P}(\mathbf{G}_{i,j} = 1 \wedge \mathbf{G}_{l,k} = 1) = \sigma(\mathbf{K}_{i,j}/T)\sigma(\mathbf{K}_{l,k}/T). \quad (5)$$

The above lemma allows us to, given some kernel matrix driven by an assumption on similarity over our data points, K , evaluate the performance of an representation model providing another kernel matrix M .

Theorem 3.6. Given a kernel matrix \mathbf{K} and associated Gibbs measure $\mu_{\mathbf{K}}$, and another kernel matrix \mathbf{M} , we can compute the expectation of $\text{Tr}(\mathbf{MG})$ as follows,

$$\mathbb{E}_{\mathbf{G} \sim \mu_{\mathbf{K}}} [\text{Tr}(\mathbf{MG})] = \sum_{1 \leq i, j \leq n} \mathbf{M}_{i,j} \mathbb{P}_{\mathbf{G} \sim \mu_{\mathbf{K}}} (\mathbf{G}_{i,j} = 1) = \sum_{1 \leq i, j \leq n} \mathbf{M}_{i,j} \sigma(\mathbf{K}_{i,j}/T). \quad (6)$$

Furthermore, the variance satisfies,

$$\text{Var}(\text{Tr}(\mathbf{MG})) = \sum_{1 \leq i, j \leq n} \mathbf{M}_{i,j}^2 \sigma(\mathbf{K}_{i,j}/T)(1 - \sigma(\mathbf{K}_{i,j}/T)).$$

We will note that computing the mean and variance of $\text{Tr}(\mathbf{MG})$, when \mathbf{G} is distributed according to the task prior, takes on the order of $O(N^2)$ computations for N data points.

Key Takeaway: Modeling label graphs with a Gibbs prior aligned to a backbone's feature kernel, turns the space of graphs on the data points into a tractable distribution, yielding closed form calculations of the mean and variance.

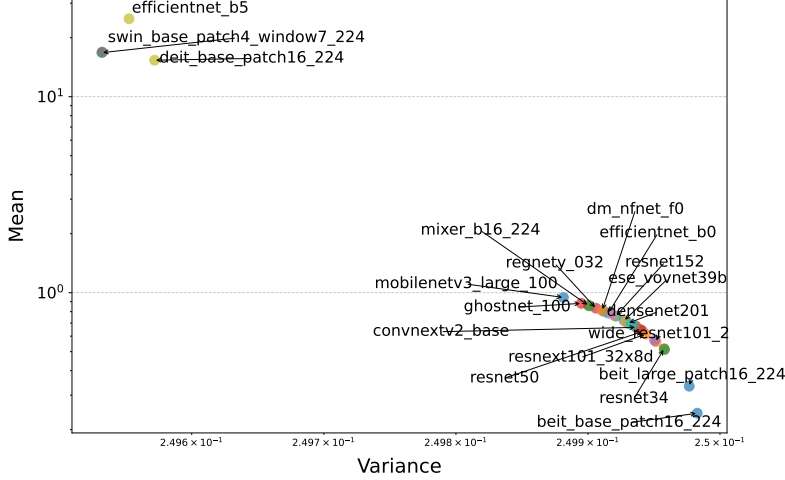


Figure 2: Here we plot the expectation and variance of $\text{Tr}(GM)$, where M is the centered cosine similarity kernel matrix for each models features generated from mini-imagenet[19], where the expectation is taken against μ_K . Here we use K as the centered cosine similarity kernel matrix for *efficientnet_b5*. Please see the appendix for more information and ablation on temperature and choice of kernel.

3.3 SSL Objectives Can Serve as Task Priors

If you don't have a prior kernel matrix, you may be able to use the same modeling assumptions you use in Self-Supervised Learning (SSL) to create an admissible kernel matrix. To start, while the above section demonstrates that supervised and SSL abide by the same objective, i.e., minimizing the absolute loss eq. (1) with \mathbf{Y} or minimizing the relative loss eq. (2) with $\mathbf{G} = \mathbf{Y}\mathbf{Y}^\top$ is equivalent, it remains to show what \mathbf{G} SSL is actually employing.

We recall that in a typical SSL setting, each sample is augmented V times to form V views. Hence we now have $\mathbf{G} \in \mathbb{R}^{NV \times NV}$. And the loss aims at collapsing together the views of each sample, i.e., $(\mathbf{G})_{i,j} = 1_{\{\lfloor i/V \rfloor = \lfloor j/V \rfloor\}}$, assuming that the data samples are ordered based on their index first, and augmentations second. The question that naturally arises is about the underlying \mathbf{Y} that the loss is considering. We formalize that result below.

Proposition 3.7. *The SSL graph given by $(\mathbf{G})_{i,j} = 1_{\{\lfloor i/V \rfloor = \lfloor j/V \rfloor\}}$ is recovered from considering the labels $\mathbf{Y} \in \mathbb{R}^{NV \times N}$ with $(\mathbf{Y})_{n,j} = 1_{\{\lfloor n/V \rfloor = 1\}}$.*

That is, SSL is implicitly acting on a labeling of the dataset that attributes to each sample a unique class. As such a labeling forces the model to maintain information about all its training samples—at least enough to separate them— it is clear that this is what maximized the Mutual Information between the original data \mathbf{X} and the final learned representation $f_\theta(\mathbf{X})$ [20]. So, we can use this *graph* \mathbf{G} as the *kernel* matrix to be our task prior.

3.4 Evaluating Model Kernels

We can use the equations in 3.6 as a way to evaluate model performance in a very fast way, i.e. without training any probes, or even assembling a collection of tasks / benchmarks. We demonstrate this in Figure 2 on a selection of models from *timm* and on a subset of 8,192 images from *mini-imagenet* [19]. We use the centered cosine similarity as the choice of kernel matrix here and in the rest of the experiments in this paper. We find that the mean and variance are negatively correlated, implying that models that perform well on average tend also to perform better across a variety of tasks. From the selection of models we tested, we find that *efficientnet* [22] performs the best, even beating more modern vision transformers [6].

4 Applications of Task Priors

4.1 Empirically Sampling Tasks for Evaluation

Starting from the task-prior distribution $\mu_{\mathbf{K}}$ over graphs introduced in the previous section, we can view every edge as an independent Bernoulli variable whose success probability is $\sigma(\mathbf{K}_{i,j}/T)$. However, for the purpose of measuring performance of a model with linear probes, we may instead want to sample from the probability measure restricted on those graphs \mathbf{G} which arise from one hot labelings \mathbf{Y} , where $\mathbf{G} = \mathbf{Y}\mathbf{Y}^\top$. We will denote by $\mu_{\mathbf{K}}^q$ the probability measure given by,

$$\mu_{\mathbf{K}}^q(G) \propto \begin{cases} \mu_{\mathbf{K}}(\mathbf{G}) & \text{if } \mathbf{G} = \mathbf{Y}\mathbf{Y}^\top \text{ for some one-hot } \mathbf{Y} \in \{0, 1\}^{N \times q} \\ 0 & \text{else} \end{cases}.$$

Sampling from the restricted measure $\mu_{\mathbf{K}}^q$ is a much more challenging problem, and ends up being equivalent to sampling from the so-called Pott's Model from statistical mechanics [28]. For instance, for binary labelings there are 2^n possible states, so sampling and computing the partition function can be completely intractable. We could use Markov Chain Monte Carlo (MCMC) methods such as the Metropolis-Hastings algorithm to sample from this distribution, but this can also prove to be challenging in practice and requires proper tuning of some parameters to get right. Instead, we propose an approximate sampling algorithm in $O(n)$ time to sample a labeling on n data points.

Suppose we write the labeling $\mathbf{Y} = [y_1, \dots, y_n]$, and we denote by \mathbf{c} a one hot vector corresponding to class c . We operate sequentially, assigning a label to each new data point we see using the following approximation of the true measure $\mu_{\mathbf{K}}^q$, where $p(y_i = \mathbf{c} | y_1, \dots, y_{i-1}) \approx \frac{1}{C} \exp\left(\frac{1}{T} \sum_{j < i} \mathbf{K}_{i,j} \mathbf{1}_{\{y_j = \mathbf{c}\}}\right)$. We can then achieve an algorithmic speedup by using the factorization of our kernel matrix as $\mathbf{K} = \mathbf{Z}\mathbf{Z}^\top$ (if we do not have access to the features, we can use for instance a Cholesky factorization here). Then we have,

$$\exp\left(\frac{1}{T} \sum_{j < i} \mathbf{K}_{i,j} \mathbf{1}_{\{y_j = \mathbf{c}\}}\right) = \exp\left(\frac{1}{T} \mathbf{Z}_i \sum_{j < i} \mathbf{Z}_j \mathbf{1}_{\{y_j = \mathbf{c}\}}\right). \quad (7)$$

From (7), we can devise our method for the sampling Algorithm 1. Using this algorithm, we are able to quickly sample labelings of the data points according to the task prior, as demonstrated in Figure 1.

Key Takeaway: An $O(N)$ prefix-sampler lets us quickly realistic downstream tasks from the Task Prior, sidestepping costly MCMC and manual benchmark curation.

Algorithm 1 Prefix Sampler for Multi-Class Task Prior

```

Require:  $\mathbf{Z} \in \mathbb{R}^{n \times r}$  ▷ factor so  $\mathbf{K} \approx \mathbf{Z}\mathbf{Z}^\top$ 
Require:  $T > 0$  ▷ temperature
Require:  $q \in \mathbb{N}$  ▷ number of classes
Ensure:  $\text{labels} \in \{0, \dots, q-1\}^n$ 
1: allocate  $\text{labels}[1:n]$  ▷ class-wise prefix sums
2:  $\mathbf{U} \leftarrow 0_{r \times q}$  ▷ length  $q$  vector
3: for  $i = 1 \dots n$  do ▷ stabilize
4:    $h \leftarrow \left(\frac{1}{T}\right) (\mathbf{Z}[i, :] \mathbf{U})$ 
5:    $h \leftarrow h - \max(h)$ 
6:    $p \leftarrow \exp(h); \quad p \leftarrow p / \sum p$ 
7:    $c \sim \text{CategoricalSample}(p)$ 
8:    $\text{labels}[i] \leftarrow c$ 
9:    $\mathbf{U}[:, c] += \mathbf{Z}_{i,:}$ 
10: end for
11: return  $\text{labels}$ 

```

4.2 Evaluating Models on Sampled Tasks

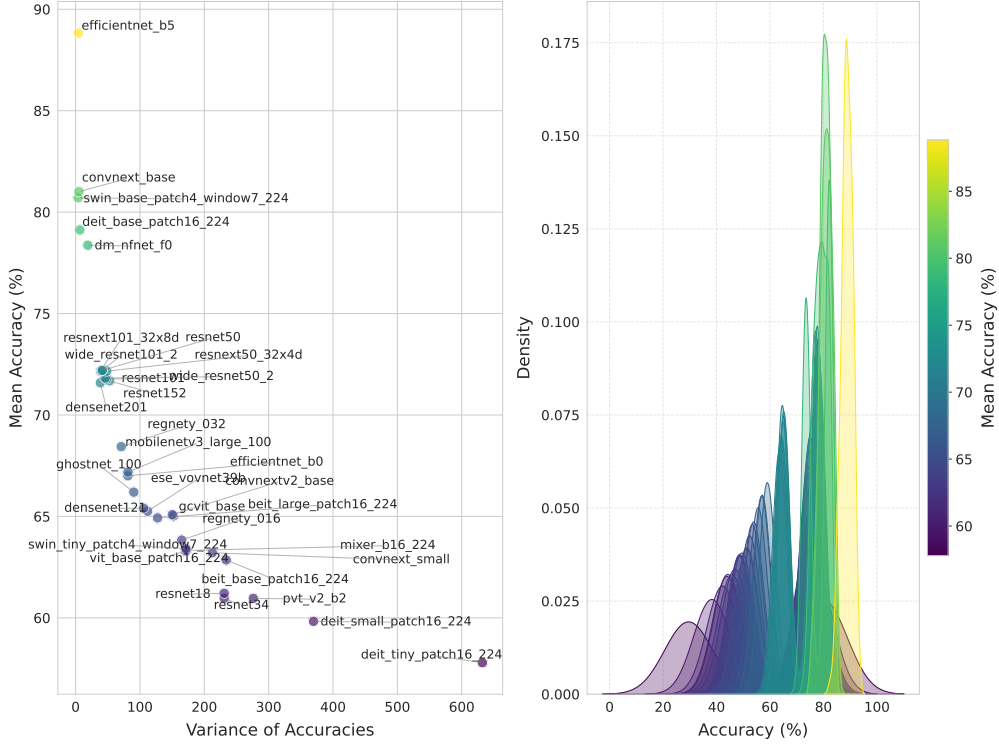


Figure 3: Linear probe performance of a selection of models from *timm* on a distribution of binary labels sampled by the *task prior* on the mini-Imagenet dataset. Here we use *efficientnet_b5* as the backbone model for the task prior distribution.

Using a selection of 33 models from *timm* [27], we are able to evaluate each model on a distribution of tasks generated using *efficientnet_b5* as our backbone prior. We report the results of this study in Figure 3, where we find that models that perform better on average also tend to have a better variance over tasks. This is a finding we will corroborate by directly measuring $\mathbb{E}_{\mu_K}[\text{Tr}(GK)]$ and $\text{Var}(\text{Tr}(GK))$ in Figure 3.

We note that the expectation and variance of $\text{Tr}(GK)$ as shown in Figure 2, tends to exhibit the same trends as the models linear probe performance on sampled tasks, as seen in Figure 3, where stronger models tend to have a higher average accuracy / trace, as well as a lower variance. We compute the correlation between these sets of data points in Figure 4.

5 Discussion

Our results establish *Task Priors* as a principled bridge between intrinsic evaluations of representation learning models and the costly practice of curating ever-larger suites of downstream benchmarks. By casting the space of tasks as a distribution over label graphs, we obtain closed-form expressions for the *expected* performance and its *variance* across all possible tasks, and we show that these statistics align with empirical linear probe performance on ImageNet-derived data. Beyond evaluation, the theory suggests a prior-aware fine-tuning objective that simultaneously maximizes mean task performance while minimizing its dispersion.

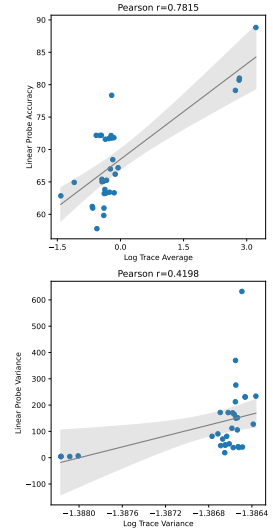


Figure 4: Correlation between the mean and variance of $\text{Tr}(GK)$ and the performance of linear probes on the same representations, with 95% confidence intervals.

5.1 Limitations and Future Work

Despite these advances, several open issues remain. While the trace metrics correlate with probe accuracy, the correlation is not exact; closing this theory–practice gap will require a deeper empirical and theoretic study. Additionally, storing the full n^2 kernel is can be prohibitive for very large datasets, although the matrices we observe are highly structured; further leveraging sparsity and low-rank factorizations is an immediate direction for further work. Our analysis is domain-agnostic, but its effectiveness on understanding the representations of Large Language Models [21], and, more generally, in natural language processing remains to be demonstrated. Our preliminary experiments hint that optimizing for the expected trace and its variance is beneficial, yet a full exploration of architectures, hyper-parameters, and interaction with existing self-supervised objectives is still outstanding. Tackling these questions will not only sharpen the foundations introduced here but may also lead to AI systems that perform *consistently well* across the vast landscape of tasks encountered in practice.

References

- [1] Philip Bachman, R. Devon Hjelm, and William Buchwalter. Learning representations by maximizing mutual information across views. In *Advances in Neural Information Processing Systems 32*, pages 15535–15545. Curran Associates, 2019.
- [2] Mathilde Caron, Ishan Misra, Julien Mairal, Priya Goyal, Piotr Bojanowski, and Armand Joulin. Unsupervised learning of visual features by contrasting cluster assignments. *CoRR*, abs/2006.09882, 2020. NeurIPS 2020.
- [3] Ting Chen, Simon Kornblith, Mohammad Norouzi, and Geoffrey Hinton. A simple framework for contrastive learning of visual representations. In *Proceedings of the 37th International Conference on Machine Learning*, volume 119 of *Proceedings of Machine Learning Research*, pages 1597–1607. PMLR, 2020.
- [4] Xinlei Chen, Haoqi Fan, Ross Girshick, and Kaiming He. Improved baselines with momentum contrastive learning. *CoRR*, abs/2003.04297, 2020.
- [5] Nello Cristianini, John Shawe-Taylor, André Elisseeff, and Jaz Kandola. On kernel-target alignment. In T. Dietterich, S. Becker, and Z. Ghahramani, editors, *Advances in Neural Information Processing Systems*, volume 14. MIT Press, 2001.
- [6] Alexey Dosovitskiy, Lucas Beyer, Alexander Kolesnikov, Dirk Weissenborn, Xiaohua Zhai, Thomas Unterthiner, Mostafa Dehghani, Matthias Minderer, Georg Heigold, Sylvain Gelly, Jakob Uszkoreit, and Neil Houlsby. An image is worth 16x16 words: Transformers for image recognition at scale, 2021.
- [7] Quentin Garrido, Randall Balestrieri, Laurent Najman, and Yann Lecun. Rankme: Assessing the downstream performance of pretrained self-supervised representations by their rank. In *International conference on machine learning*, pages 10929–10974. PMLR, 2023.
- [8] Arthur Gretton, Kenji Fukumizu, Choon Teo, Le Song, Bernhard Schölkopf, and Alex Smola. A kernel statistical test of independence. In J. Platt, D. Koller, Y. Singer, and S. Roweis, editors, *Advances in Neural Information Processing Systems*, volume 20. Curran Associates, Inc., 2007.
- [9] Kaiming He, Haoqi Fan, Yuxin Wu, Saining Xie, and Ross Girshick. Momentum contrast for unsupervised visual representation learning. In *Proc. IEEE/CVF Conf. on Computer Vision and Pattern Recognition*, pages 9729–9738, 2020.
- [10] Olivier Henaff. Data-efficient image recognition with contrastive predictive coding. In *Proceedings of the 37th International Conference on Machine Learning*, volume 119 of *Proceedings of Machine Learning Research*, pages 4182–4192. PMLR, 2020.
- [11] Jeremy Howard. Imagenette: A smaller subset of 10 easily classified classes from imagenet, March 2019.

[12] Quentin Lhoest, Albert Villanova del Moral, Yacine Jernite, Abhishek Thakur, Patrick von Platen, Suraj Patil, Julien Chaumond, Mariama Drame, Julien Plu, Lewis Tunstall, Joe Davison, Mario Šaško, Gunjan Chhablani, Bhavitya Malik, Simon Brandeis, Teven Le Scao, Victor Sanh, Canwen Xu, Nicolas Patry, Angelina McMillan-Major, Philipp Schmid, Sylvain Gugger, Clément Delangue, Théo Matussière, Lysandre Debut, Stas Bekman, Pierrick Cistac, Thibault Goehringer, Victor Mustar, François Lagunas, Alexander Rush, and Thomas Wolf. Datasets: A community library for natural language processing. In Heike Adel and Shuming Shi, editors, *Proceedings of the 2021 Conference on Empirical Methods in Natural Language Processing: System Demonstrations*, pages 175–184, Online and Punta Cana, Dominican Republic, November 2021. Association for Computational Linguistics.

[13] Xinhao Li, Zhenpeng Huang, Jing Wang, Kunchang Li, and Limin Wang. Videoeval: Comprehensive benchmark suite for low-cost evaluation of video foundation model, 2024.

[14] Yazhe Li, Roman Pogodin, Danica J. Sutherland, and Arthur Gretton. Self-supervised learning with kernel dependence maximization, 2021.

[15] Percy Liang, Rishi Bommasani, Tony Lee, Dimitris Tsipras, Dilara Soylu, Michihiro Yasunaga, Yian Zhang, Deepak Narayanan, Yuhuai Wu, Ananya Kumar, Benjamin Newman, Binhang Yuan, Bobby Yan, Ce Zhang, Christian Cosgrove, Christopher D. Manning, Christopher Ré, Diana Acosta-Navas, Drew A. Hudson, Eric Zelikman, Esin Durmus, Faisal Ladhak, Frieda Rong, Hongyu Ren, Huaxiu Yao, Jue Wang, Keshav Santhanam, Laurel Orr, Lucia Zheng, Mert Yuksekgonul, Mirac Suzgun, Nathan Kim, Neel Guha, Niladri Chatterji, Omar Khattab, Peter Henderson, Qian Huang, Ryan Chi, Sang Michael Xie, Shibani Santurkar, Surya Ganguli, Tatsunori Hashimoto, Thomas Icard, Tianyi Zhang, Vishrav Chaudhary, William Wang, Xuechen Li, Yifan Mai, Yuhui Zhang, and Yuta Koreeda. Holistic evaluation of language models, 2023.

[16] Tsung-Yi Lin, Michael Maire, Serge Belongie, James Hays, Pietro Perona, Deva Ramanan, Piotr Dollár, and C Lawrence Zitnick. Microsoft coco: Common objects in context. In *Computer vision–ECCV 2014: 13th European conference, zurich, Switzerland, September 6–12, 2014, proceedings, part v 13*, pages 740–755. Springer, 2014.

[17] Markus Marks, Manuel Knott, Neehar Kondapaneni, Elijah Cole, Thijs Defraeye, Fernando Perez-Cruz, and Pietro Perona. A Closer Look at Benchmarking Self-supervised Pre-training with Image Classification. *International Journal of Computer Vision*, April 2025.

[18] Niklas Muennighoff, Nouamane Tazi, Loïc Magne, and Nils Reimers. Mteb: Massive text embedding benchmark, 2023.

[19] Olga Russakovsky, Jia Deng, Hao Su, Jonathan Krause, Sanjeev Satheesh, Sean Ma, Zhiheng Huang, Andrej Karpathy, Aditya Khosla, Michael Bernstein, Alexander C. Berg, and Li Fei-Fei. ImageNet Large Scale Visual Recognition Challenge. *International Journal of Computer Vision (IJCV)*, 115(3):211–252, 2015.

[20] Ravid Shwartz-Ziv and Yann LeCun. To compress or not to compress- self-supervised learning and information theory: A review, 2023.

[21] Oscar Skean, Md Rifat Arefin, Dan Zhao, Niket Patel, Jalal Naghiyev, Yann LeCun, and Ravid Shwartz-Ziv. Layer by layer: Uncovering hidden representations in language models. *arXiv preprint arXiv:2502.02013*, 2025.

[22] Mingxing Tan and Quoc Le. Efficientnet: Rethinking model scaling for convolutional neural networks. In *International conference on machine learning*, pages 6105–6114. PMLR, 2019.

[23] Vimal Thilak, Chen Huang, Omid Saremi, Laurent Dinh, Hanlin Goh, Preetum Nakkiran, Joshua M Susskind, and Etai Littwin. Lidar: Sensing linear probing performance in joint embedding ssl architectures. *arXiv preprint arXiv:2312.04000*, 2023.

[24] Aaron van den Oord, Yazhe Li, and Oriol Vinyals. Representation learning with contrastive predictive coding. *CoRR*, abs/1807.03748, 2018.

[25] Alex Wang, Amanpreet Singh, Julian Michael, Felix Hill, Omer Levy, and Samuel R Bowman. Glue: A multi-task benchmark and analysis platform for natural language understanding. *arXiv preprint arXiv:1804.07461*, 2018.

- [26] Tongzhou Wang and Phillip Isola. Understanding contrastive representation learning through alignment and uniformity on the hypersphere. In *Proceedings of the 37th International Conference on Machine Learning*, volume 119 of *Proceedings of Machine Learning Research*, pages 9929–9939. PMLR, 2020.
- [27] Ross Wightman. Pytorch image models. <https://github.com/rwightman/pytorch-image-models>, 2019.
- [28] F. Y. Wu. The potts model. *Rev. Mod. Phys.*, 54:235–268, Jan 1982.
- [29] Jure Zbontar, Li Jing, Ishan Misra, Yann LeCun, and Stéphane Deny. Barlow twins: Self-supervised learning via redundancy reduction. In *Proceedings of the 38th International Conference on Machine Learning*, volume 139 of *Proceedings of Machine Learning Research*, pages 12310–12320. PMLR, 2021.
- [30] Xiaohua Zhai, Joan Puigcerver, Alexander Kolesnikov, Pierre Ruyssen, Carlos Riquelme, Mario Lucic, Josip Djolonga, Andre Susano Pinto, Maxim Neumann, Alexey Dosovitskiy, Lucas Beyer, Olivier Bachem, Michael Tschannen, Marcin Michalski, Olivier Bousquet, Sylvain Gelly, and Neil Houlsby. A large-scale study of representation learning with the visual task adaptation benchmark, 2020.

A Main Theoretical Results

A.1 Proof of theorem 3.3

Proof. The proof will involve a few different steps. First, we will solve the optimization objective $\mathcal{L}(\mathbf{W}, \mathbf{b}, \theta)$ for \mathbf{b} and then for \mathbf{W} .

Solving for \mathbf{b} . Let's first solve for the bias \mathbf{b} directly since the loss is convex in \mathbf{b}

$$\begin{aligned} & \nabla_{\mathbf{b}} \mathcal{L}(\mathbf{W}, \mathbf{b}, \theta) = \mathbf{0} \\ \iff & \nabla_{\mathbf{b}} \frac{1}{N} \|\mathbf{W}f_{\theta}(\mathbf{X}) + \mathbf{b}\mathbf{1}_N^\top - \mathbf{Y}\|_F^2 = \mathbf{0} \\ \implies & \frac{2}{N} (\mathbf{W}f_{\theta}(\mathbf{X}) + \mathbf{b}\mathbf{1}_N^\top - \mathbf{Y}) \mathbf{1}_N = \mathbf{0} \\ \iff & \mathbf{W}f_{\theta}(\mathbf{X})\mathbf{1}_N + \mathbf{b}N - \mathbf{Y}\mathbf{1}_N = \mathbf{0} \\ \iff & \mathbf{b} = \frac{1}{N} \mathbf{Y}\mathbf{1}_N - \frac{1}{N} \mathbf{W}f_{\theta}(\mathbf{X})\mathbf{1}_N. \end{aligned}$$

From that we can simplify the loss by injecting the optimal value of the bias parameter as

$$\begin{aligned} \min_{\mathbf{b}} \mathcal{L}(\mathbf{W}, \mathbf{b}, \theta) &= \min_{\mathbf{b}} \frac{1}{N} \|\mathbf{W}f_{\theta}(\mathbf{X}) + \mathbf{b}\mathbf{1}_N^\top - \mathbf{Y}\|_F^2 \\ &= \frac{1}{N} \left\| \mathbf{W}f_{\theta}(\mathbf{X}) + \left(\frac{1}{N} \mathbf{Y}\mathbf{1}_N - \frac{1}{N} \mathbf{W}f_{\theta}(\mathbf{X})\mathbf{1}_N \right) \mathbf{1}_N^\top - \mathbf{Y} \right\|_F^2 \\ &= \frac{1}{N} \|\mathbf{W}f_{\theta}(\mathbf{X})\mathbf{H} - \mathbf{Y}\mathbf{H}\|_F^2 \end{aligned}$$

with \mathbf{H} the centering matrix $\mathbf{H} \triangleq \mathbf{I} - \frac{1}{N} \mathbf{1}_N \mathbf{1}_N^\top$.

Solving for \mathbf{W} . Similarly to the derivation for \mathbf{b} , we can now optimize for \mathbf{W} again using the fact that the loss is convex in \mathbf{W} leading to the following

$$\begin{aligned} & \nabla_{\mathbf{W}} \min_{\mathbf{b}} \mathcal{L}(\mathbf{W}, \mathbf{b}, \theta) = \mathbf{0} \\ \iff & \nabla_{\mathbf{W}} \frac{1}{N} \|\mathbf{W}f_{\theta}(\mathbf{X})\mathbf{H} - \mathbf{Y}\mathbf{H}\|_F^2 = \mathbf{0} \\ \implies & 2 \frac{1}{N} \mathbf{W}f_{\theta}(\mathbf{X})\mathbf{H}f_{\theta}(\mathbf{X})^\top - 2 \frac{1}{N} \mathbf{Y}\mathbf{H}f_{\theta}(\mathbf{X})^\top = \mathbf{0} \\ \iff & \mathbf{W} = \mathbf{Y}\mathbf{H}f_{\theta}(\mathbf{X})^\top (f_{\theta}(\mathbf{X})\mathbf{H}f_{\theta}(\mathbf{X})^\top)^{-1} \end{aligned}$$

from which we can again further simplify the loss as follows

$$\begin{aligned} \min_{\mathbf{W}, \mathbf{b}} \mathcal{L}(\mathbf{W}, \mathbf{b}, \theta) &= \min_{\mathbf{W}} \frac{1}{N} \|\mathbf{W}f_{\theta}(\mathbf{X})\mathbf{H} - \mathbf{Y}\mathbf{H}\|_F^2 \\ &= \frac{1}{N} \left\| (\mathbf{Y}\mathbf{H}f_{\theta}(\mathbf{X})^\top) (f_{\theta}(\mathbf{X})\mathbf{H}f_{\theta}(\mathbf{X})^\top)^{-1} f_{\theta}(\mathbf{X})\mathbf{H} - \mathbf{Y}\mathbf{H} \right\|_F^2 \\ &= \frac{1}{N} \|\mathbf{Y}\mathbf{V}\mathbf{S}^\top (\mathbf{S}\mathbf{S}^\top)^{-1} \mathbf{S}\mathbf{V}^\top - \mathbf{Y}\mathbf{H}\|_F^2 \end{aligned}$$

where we used the singular value decomposition $\mathbf{U}\mathbf{S}\mathbf{V}^\top$ of $f_{\theta}(\mathbf{X})\mathbf{H}$. We will now do some algebraic manipulations to simplify the above as follows

$$\begin{aligned} \min_{\mathbf{W}, \mathbf{b}} \mathcal{L}(\mathbf{W}, \mathbf{b}, \theta) &= \frac{1}{N} \|\mathbf{Y}\mathbf{H}\|_F^2 - 2 \frac{1}{N} \text{Tr} (\mathbf{H}^\top \mathbf{Y}^\top \mathbf{Y}\mathbf{V}\mathbf{S}^\top (\mathbf{S}\mathbf{S}^\top)^{-1} \mathbf{S}\mathbf{V}^\top) \\ &\quad + \frac{1}{N} \text{Tr} (\mathbf{V}^\top \mathbf{Y}^\top \mathbf{Y}\mathbf{V}\mathbf{S}^\top (\mathbf{S}\mathbf{S}^\top)^{-1} \mathbf{S}) \end{aligned}$$

Now we use the fact that $\mathbf{V}^\top \mathbf{H} = \mathbf{V}^\top$ whenever the SVD was done on the centered \mathbf{X} (which is the case here) to further simplify

$$\begin{aligned} \min_{\mathbf{W}, \mathbf{b}} \mathcal{L}(\mathbf{W}, \mathbf{b}, \theta) &= \frac{1}{N} \|\mathbf{YH}\|_F^2 - 2 \frac{1}{N} \text{Tr}(\mathbf{V}^\top \mathbf{Y}^\top \mathbf{YV} (\mathbf{S}^2)^{-1} \mathbf{S}^2) \\ &\quad + \frac{1}{N} \text{Tr}(\mathbf{V}^\top \mathbf{Y}^\top \mathbf{YV} (\mathbf{S}^2)^{-2} \mathbf{S}^4) \\ &= \frac{1}{N} \|\mathbf{YH}\|_F^2 - 2 \frac{1}{N} \text{Tr}(\mathbf{V}^\top \mathbf{Y}^\top \mathbf{YV}) + \frac{1}{N} \text{Tr}(\mathbf{V}^\top \mathbf{Y}^\top \mathbf{YV}) \\ &= \frac{1}{N} \|\mathbf{YH}\|_F^2 - \frac{1}{N} \text{Tr}(\mathbf{V}^\top \mathbf{Y}^\top \mathbf{YV}), \end{aligned}$$

as desired. \square

A.2 Proof of lemma 3.5

Proof. Recall that $\mu(\mathbf{G}) = \frac{1}{Z_{T, \mathbf{K}}} e^{\frac{1}{T} \text{Tr}(\mathbf{GK})}$. Then we can compute that,

$$\begin{aligned} \mathbb{P}(\mathbf{G}_{i,j} = 1) &= \mathbb{E}_\mu[\mathbf{G}_{i,j}] \\ &= \frac{1}{Z_{T, \mathbf{K}}} \sum_{\mathbf{G}: \mathbf{G}_{i,j}=1} e^{\frac{1}{T} \text{Tr}(\mathbf{GK})} \\ &= \frac{1}{Z_{T, \mathbf{K}}} \sum_{\mathbf{G}: \mathbf{G}_{i,j}=1} e^{\frac{1}{T} \sum_{i,j=1}^n \mathbf{G}_{i,j} \mathbf{K}_{i,j}} \\ &= \frac{1}{Z_{T, \mathbf{K}}} \sum_{\mathbf{G}: \mathbf{G}_{i,j}=1} \left[\prod_{1 \leq k, l \leq n} e^{\frac{1}{T} \mathbf{K}_{k,l} \mathbf{G}_{k,l}} \right]. \end{aligned}$$

Now notice we can let:

$$\begin{aligned} w_1 &= \sum_{\mathbf{G}: \mathbf{G}_{i,j}=1} \left[\prod_{1 \leq k, l \leq n} e^{\frac{1}{T} \mathbf{K}_{k,l} \mathbf{G}_{k,l}} \right], \\ w_0 &= \sum_{\mathbf{G}: \mathbf{G}_{i,j}=0} \left[\prod_{1 \leq k, l \leq n} e^{\frac{1}{T} \mathbf{K}_{k,l} \mathbf{G}_{k,l}} \right]. \end{aligned}$$

And then,

$$\mathbb{P}(\mathbf{G}_{i,j} = 1) = \frac{w_1}{w_0 + w_1}.$$

Notice though that we can write,

$$\sum_{\mathbf{G}: \mathbf{G}_{i,j}=1} \left[\prod_{1 \leq k, l \leq n} e^{\frac{1}{T} \mathbf{K}_{k,l} \mathbf{G}_{k,l}} \right] = e^{\frac{1}{T} \mathbf{K}_{i,j}} \sum_{\mathbf{G}: \mathbf{G}_{i,j}=0} \left[\prod_{1 \leq k, l \leq n} e^{\frac{1}{T} \mathbf{K}_{k,l} \mathbf{G}_{k,l}} \right].$$

So,

$$w_1 = e^{\frac{1}{T} \mathbf{K}_{i,j}} \cdot w_0.$$

Then we know that,

$$\mathbb{P}(\mathbf{G}_{i,j} = 1) = \frac{e^{\frac{1}{T} \mathbf{K}_{i,j}} \cdot w_0}{w_0 + e^{\frac{1}{T} \mathbf{K}_{i,j}} \cdot w_0} = \frac{e^{\frac{\mathbf{K}_{i,j}}{T}}}{1 + e^{\frac{\mathbf{K}_{i,j}}{T}}} = \sigma\left(\frac{\mathbf{K}_{i,j}}{T}\right).$$

For the second part, we want to compute $\mathbb{P}(\mathbf{G}_{i,j}\mathbf{G}_{l,k} = 1)$, which we can note is clearly equivalent to $\mathbb{P}(\mathbf{G}_{i,j} = 1 \wedge \mathbf{G}_{l,k} = 1)$. As before, we can compute,

$$\begin{aligned}\mathbb{P}(\mathbf{G}_{i,j}\mathbf{G}_{l,k} = 1) &= \mathbb{E}_\mu[\mathbf{G}_{i,j}\mathbf{G}_{l,k}] \\ &= \frac{1}{Z_{T,\mathbf{K}}} \sum_{\mathbf{G}: \mathbf{G}_{i,j}\mathbf{G}_{l,k}=1} e^{\frac{1}{T} \text{Tr}(\mathbf{G}\mathbf{K})} \\ &= \frac{1}{Z_{T,\mathbf{K}}} \sum_{\mathbf{G}: \mathbf{G}_{i,j}\mathbf{G}_{l,k}=1} e^{\frac{1}{T} \sum_{i,j=1}^n \mathbf{G}_{i,j}\mathbf{K}_{i,j}} \\ &= \frac{1}{Z_{T,\mathbf{K}}} \sum_{\mathbf{G}: \mathbf{G}_{i,j}\mathbf{G}_{l,k}=1} \left[\prod_{1 \leq k, l \leq n} e^{\frac{1}{T} \mathbf{K}_{k,l} \mathbf{G}_{k,l}} \right].\end{aligned}$$

We then let,

$$\begin{aligned}w_1 &= \sum_{\mathbf{G}: \mathbf{G}_{i,j}\mathbf{G}_{l,k}=1} \left[\prod_{1 \leq k, l \leq n} e^{\frac{1}{T} \mathbf{K}_{k,l} \mathbf{G}_{k,l}} \right], \\ w_0 &= \sum_{\mathbf{G}: \mathbf{G}_{i,j}\mathbf{G}_{l,k}=0} \left[\prod_{1 \leq k, l \leq n} e^{\frac{1}{T} \mathbf{K}_{k,l} \mathbf{G}_{k,l}} \right].\end{aligned}$$

Which, we can note if $(i, j) \neq (l, k)$, then we have:

$$\begin{aligned}w_0 &= \sum_{\mathbf{G}: \mathbf{G}_{i,j}\mathbf{G}_{l,k}=0} \left[\prod_{1 \leq k, l \leq n} e^{\frac{1}{T} \mathbf{K}_{k,l} \mathbf{G}_{k,l}} \right] \\ &= \sum_{\mathbf{G}: \mathbf{G}_{i,j}=0, \mathbf{G}_{l,k}=0} \left[\prod_{1 \leq k, l \leq n} e^{\frac{1}{T} \mathbf{K}_{k,l} \mathbf{G}_{k,l}} \right] + \sum_{\mathbf{G}: \mathbf{G}_{i,j}=0, \mathbf{G}_{l,k}=1} \left[\prod_{1 \leq k, l \leq n} e^{\frac{1}{T} \mathbf{K}_{k,l} \mathbf{G}_{k,l}} \right] \\ &\quad + \sum_{\mathbf{G}: \mathbf{G}_{i,j}=1, \mathbf{G}_{l,k}=0} \left[\prod_{1 \leq k, l \leq n} e^{\frac{1}{T} \mathbf{K}_{k,l} \mathbf{G}_{k,l}} \right] \\ &= (e^{\frac{1}{T}(\mathbf{K}_{i,j} + \mathbf{K}_{l,k})})^{-1} \sum_{\mathbf{G}: \mathbf{G}_{i,j}=1, \mathbf{G}_{l,k}=1} \left[\prod_{1 \leq k, l \leq n} e^{\frac{1}{T} \mathbf{K}_{k,l} \mathbf{G}_{k,l}} \right] \\ &\quad + (e^{\frac{1}{T}\mathbf{K}_{i,j}})^{-1} \sum_{\mathbf{G}: \mathbf{G}_{i,j}=1, \mathbf{G}_{l,k}=1} \left[\prod_{1 \leq k, l \leq n} e^{\frac{1}{T} \mathbf{K}_{k,l} \mathbf{G}_{k,l}} \right] \\ &\quad + (e^{\frac{1}{T}\mathbf{K}_{l,k}})^{-1} \sum_{\mathbf{G}: \mathbf{G}_{i,j}=1, \mathbf{G}_{l,k}=1} \left[\prod_{1 \leq k, l \leq n} e^{\frac{1}{T} \mathbf{K}_{k,l} \mathbf{G}_{k,l}} \right] \\ &= (e^{-\frac{1}{T}(\mathbf{K}_{i,j} + \mathbf{K}_{l,k})} + e^{-\frac{1}{T}\mathbf{K}_{i,j}} + e^{-\frac{1}{T}\mathbf{K}_{l,k}}) \sum_{\mathbf{G}: \mathbf{G}_{i,j}=1, \mathbf{G}_{l,k}=1} \left[\prod_{1 \leq k, l \leq n} e^{\frac{1}{T} \mathbf{K}_{k,l} \mathbf{G}_{k,l}} \right] \\ &= (e^{-\frac{1}{T}(\mathbf{K}_{i,j} + \mathbf{K}_{l,k})} + e^{-\frac{1}{T}\mathbf{K}_{i,j}} + e^{-\frac{1}{T}\mathbf{K}_{l,k}}) w_1.\end{aligned}$$

Then we can write that,

$$w_0 + w_1 = (1 + e^{-\frac{1}{T}(\mathbf{K}_{i,j} + \mathbf{K}_{l,k})} + e^{-\frac{1}{T}\mathbf{K}_{i,j}} + e^{-\frac{1}{T}\mathbf{K}_{l,k}}) w_1.$$

So then,

$$\begin{aligned}
\mathbb{P}(\mathbf{G}_{i,j}\mathbf{G}_{l,k} = 1) &= \frac{w_1}{w_0 + w_1} \\
&= \frac{1}{(1 + e^{-\frac{1}{T}(\mathbf{K}_{i,j} + \mathbf{K}_{l,k})} + e^{-\frac{1}{T}\mathbf{K}_{i,j}} + e^{-\frac{1}{T}\mathbf{K}_{l,k}})} \\
&= \frac{1}{(1 + e^{-\frac{1}{T}\mathbf{K}_{i,j}})(1 + e^{-\frac{1}{T}\mathbf{K}_{l,k}})} \\
&= \sigma\left(\frac{\mathbf{K}_{i,j}}{T}\right)\sigma\left(\frac{\mathbf{K}_{l,k}}{T}\right).
\end{aligned}$$

□

A.3 Proof of theorem 3.6

Proof. The first equality in the equation follows from the linearity of expectation, and the characterization that,

$$\text{Tr}(\mathbf{M}\mathbf{G}) = \sum_{1 \leq i, j \leq n} \mathbf{M}_{i,j} \mathbf{G}_{i,j},$$

for \mathbf{M}, \mathbf{G} symmetric matrices. Then, notice that this is a weighted sum of independent Bernoulli random variables. So, $\mathbb{E}_{\mathbf{G} \sim \mu_{\mathbf{K}}}[\mathbf{G}_{i,j}] = \mathbb{P}_{\mathbf{G} \sim \mu_{\mathbf{K}}}(\mathbf{G}_{i,j} = 1)$ and we can apply the above lemma and we are done.

For the second part, since this is a sum of independent random variables, we may use,

$$\text{Var}(\text{Tr}(\mathbf{M}\mathbf{G})) = \sum_{1 \leq i, j \leq n} \mathbf{M}_{i,j}^2 \text{Var}(G_{i,j}) \quad (8)$$

$$= \sum_{1 \leq i, j \leq n} \mathbf{M}_{i,j}^2 \mathbb{P}(\mathbf{G}_{i,j} = 1)(1 - \mathbb{P}(\mathbf{G}_{i,j} = 1)) \quad (9)$$

$$= \sum_{1 \leq i, j \leq n} \mathbf{M}_{i,j}^2 \sigma(\mathbf{K}_{i,j}/T)(1 - \sigma(\mathbf{K}_{i,j}/T)). \quad (10)$$

□

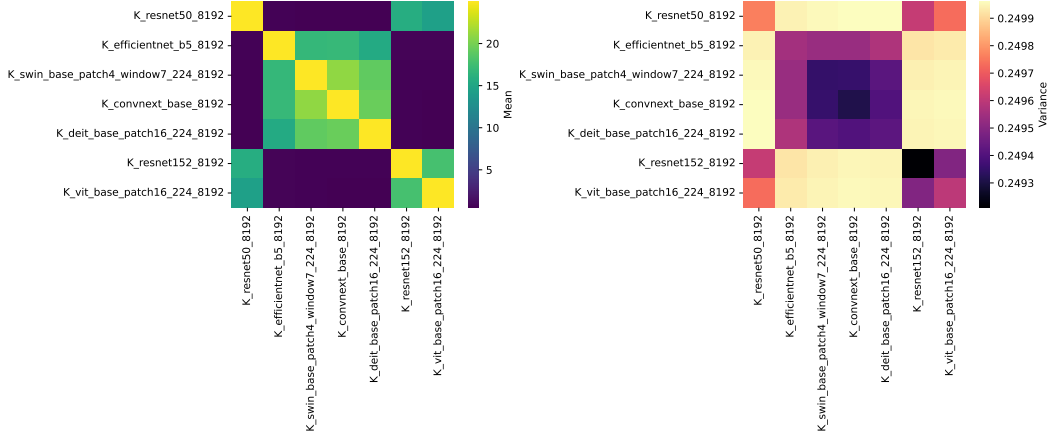


Figure 5: Here, we show a comparison of how the choice of task prior kernel \mathbf{K} , reflected here in the color of the data points, affects the the evaluation of the mean and variance of $\text{Tr}(\mathbf{M}\mathbf{G})$. Each point is computed via the exact formulas given in 3.6, with a temperature of $T = 0.01$.

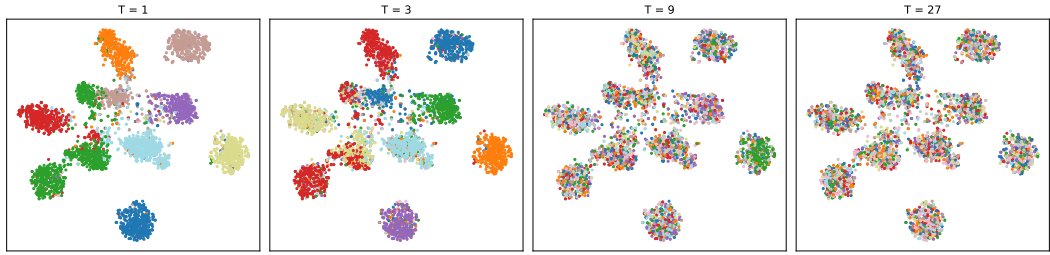


Figure 6: Here we show a TSNE plot of Imagenette, with labels generated by the sampling Algorithm 1 for four choices of temperature.

B Additional Empirical Studies

B.1 Ablation on Choice of Kernel

In Figure 5, we can see how the choice of task prior kernel matrix affects the downstream computation of the mean and variance of $\text{Tr}(\mathbf{M}\mathbf{G})$. As we might expect, we see that generally the mean $\mathbb{E}_{\mathbf{G} \sim \mu_{\mathbf{K}}}[\text{Tr}(\mathbf{M}\mathbf{G})]$ is higher when the task prior kernel \mathbf{K} matrix is the same as the the matrix being evaluated \mathbf{M} . We don't see this same behavior with the variance $\text{Var}_{\mathbf{G} \sim \mu_{\mathbf{K}}}(\text{Tr}(\mathbf{M}\mathbf{G}))$.

B.2 Ablation on the Temperature Parameter

In Figure 6, we can see the effect of the sampler changing the temperature in the measure. We can see how increasing temperature increases diversity but also brings us closer to a uniform distribution over labels.

C taskpriors PyTorch Package

Here we provide a brief demonstration of how one can use the provided codebase. We use the `analyze` function to compute the expectation and variance of a model with respect to a simple prior, as we compute in Theorem 3.6. We can also use the sampling method to sample labels as in Algorithm 1.

```
import torch
from torchvision import datasets, transforms, models
from torch.utils.data import DataLoader

from taskpriors import analyze
from taskpriors.sampler import sample_labels_from_model

# Select device
device = 'cuda' if torch.cuda.is_available() else 'cpu'

# Data transformations: resize, crop, normalize
transform = transforms.Compose([
    transforms.Resize(224),
    transforms.CenterCrop(224),
    transforms.ToTensor(),
    transforms.Normalize([0.485, 0.456, 0.406],
                        [0.229, 0.224, 0.225]),
])

# Load Imagenette training split
dataset = datasets.Imagenette(root='data',
                               split='train',
                               transform=transform,
                               download=True)
loader = DataLoader(dataset,
                     batch_size=64,
                     shuffle=False)

# Initialize ResNet-18 backbone (remove final FC layer)
model = models.resnet18(
    weights=models.ResNet18_Weights.IMGNET1K_V1
)
model.fc = torch.nn.Identity()
model = model.to(device)

# Compute dataset statistics via TaskPriors
stats = analyze(model, loader)
print(stats)

# Sample soft labels from the model
labels = sample_labels_from_model(
    model,
    loader,
    num_classes=10,
    temperature=1000.0,
    seed=0,
    device=device
)
print(labels.shape)
```